

# The $Z_3$ symmetric I(2+1)HDM

A. Aranda<sup>\*1</sup>, D. Hernández-Otero<sup>†2</sup>, J. Hernández-Sánchez<sup>‡3</sup>, S. Moretti<sup>§4</sup>,  
 D. Rojas-Ciofalo<sup>¶4</sup>, T. Shindou<sup>||5</sup>

<sup>1</sup> *Facultad de Ciencias-CUICBAS, Universidad de Colima,  
 C.P.28045, Colima, México 01000, México*

<sup>2</sup> *Instituto de Física, Benemérita Universidad Autónoma de Puebla,  
 Apdo. Postal J-48, C.P. 72570 Puebla, Puebla, México*

<sup>3</sup> *Facultad de Ciencias de la Electrónica, Benemérita Universidad Autónoma de Puebla,  
 Apdo. Postal 542, C.P. 72570 Puebla, Puebla, México*

<sup>4</sup> *School of Physics and Astronomy, University of Southampton,  
 Southampton, SO17 1BJ, United Kingdom*

<sup>5</sup> *Division of Liberal-Arts, Kogakuin University,  
 2665-1 Nakano-machi, Hachioji, Tokyo, 192-0015, Japan*

## Abstract

We introduce a 3-Higgs Doublet Model (3HDM) with two Inert (or dark) (pseudo)scalar doublets and an active Higgs one, hence termed I(2+1)HDM, in the presence of a discrete  $Z_3$  acting upon the three doublet fields. Assuming a maximally symmetric configuration of the parameters related to the two dark doublets, known in literature as ‘dark democracy’, we show that such a construct yields a two-component Dark Matter (DM) model and the two DM candidates have opposite CP parity. Herein, the most interesting solutions, those that saturate the relic density and where contributions to the latter from the two DM candidates are

---

<sup>\*</sup>E-mail: [fefo@ucol.mx](mailto:fefo@ucol.mx)

<sup>†</sup>E-mail: [danielah@ifuap.buap.mx](mailto:danielah@ifuap.buap.mx)

<sup>‡</sup>E-mail: [jaime.hernandez@correo.buap.mx](mailto:jaime.hernandez@correo.buap.mx)

<sup>§</sup>E-mail: [S.Moretti@soton.ac.uk](mailto:S.Moretti@soton.ac.uk)

<sup>¶</sup>E-mail: [D.Rojas-Ciofalo@soton.ac.uk](mailto:D.Rojas-Ciofalo@soton.ac.uk)

<sup>||</sup>E-mail: [shindou@cc.kogakuin.ac.jp](mailto:shindou@cc.kogakuin.ac.jp)

of similar magnitude, are achieved when there is a high level of degeneracy in the (dark) charged sector. In order to probe this phenomenology, we have produced a set of benchmark scenarios in the I(2+1)HDM, with the invoked  $Z_3$  symmetry, which are further compliant with (in)direct searches for DM as well as other experimental data impinging on both the dark and Higgs sectors of the model, chiefly, in the form of Electro-Weak Precision Observables (EWPOs), Standard Model (SM)-like Higgs boson measurements at the Large Hadron Collider (LHC) and void searches for additional (pseudo)scalar states at the CERN machine and previous colliders.

## 1 Introduction

The discovery of a Higgs boson by the Large Hadron Collider (LHC) in July 2012 [1, 2] has finally confirmed that Electro-Weak Symmetry Breaking (EWSB) is triggered by the Higgs mechanism. While such a new state of Nature is perfectly consistent with the Standard Model (SM), which incorporates one Higgs doublet, there is no compelling reason to assume that there should be only one. In fact, it is possible that additional Higgs doublets exist such that their corresponding Higgs bosons could be found during one of the upcoming LHC runs. If one assumes that doublet (complex) representations of Higgs fields are those chosen by Nature to implement EWSB, which is entirely plausible in the light of the fact that only such a structure is able to give mass to the  $W^\pm$  and  $Z$  bosons of the SM while preserving a massless photon, thereby in turn enabling unification of Electro-Magnetic (EM) and weak interactions, then one may wonder what can models with a generic number  $N$  of Higgs doublets, in turn defining the class of  $N$ -Higgs Doublet Models (NHDMs), produce in terms of new physics signals. The question is particularly intriguing if one further connects it to the need to explain the existence of Dark Matter (DM) in Nature, something that is absent in the SM.

In order to attempt answering such a more articulate question, one may concentrate on the class of 2-Higgs Doublet Models (2HDMs) [3]. In doing so, one should make sure to realise a 2HDM in a structure within which the DM candidate is a *stable* on cosmological time scales, *cold* (i.e., non-relativistic) at the onset of galaxy formation, *non-baryonic*, *neutral* and *weakly interacting* component of the Universe [4]. A very simple 2HDM realisation that provides a (pseudo)scalar DM candidate is the model with 1 Inert (I) doublet plus 1 Higgs (H) doublet, that we label as I(1+1)HDM. This 2HDM representation is known in the literature as the Inert Doublet Model (IDM), which was proposed in 1976 [5] and has been studied extensively over many decades. In this case, one  $SU(2)_L$  doublet with the same quantum numbers as the SM Higgs one

is introduced. Here, a  $Z_2$  symmetry is also introduced, under which the even parity is assigned to the SM Higgs doublet and the odd parity is assigned to the additional one. A possible vacuum configuration of this model is  $(v, 0)$ , where the second doublet does not develop a Vacuum Expectation Value (VEV) while the first one inherits the SM VEV,  $v^1$ . With this vacuum configuration, the  $Z_2$  symmetry remains even after EWSB. In fact, the former does not take part in EWSB while the latter is essentially the aforementioned Higgs state discovered at the CERN machine. Since the inert doublet does not couple to fermions, as it is by construction the only  $Z_2$ -odd field in the model, it provides a stable DM candidate. In essence, this is the lightest state among the two neutral (scalar and pseudoscalar) inert states with  $Z_2$ -odd quantum numbers (while all the SM states are  $Z_2$ -even)<sup>2</sup>.

The next class of NHDMs is constituted by 3-Higgs Doublet Models (3HDMs). The case for these is particularly promising for two main reasons. To begin with, 3HDMs are more tractable than higher multiplicity NHDMs as all possible finite symmetries (but not all continuous ones) have been identified [6]. Furthermore, and perhaps most intriguingly, 3HDMs may shed light on the flavor problem, namely the problem of the origin and nature of the three families of quarks and leptons, including neutrinos, and their pattern of masses, mixings and CP violation. Indeed, it is possible that the three families of SM fermions could be described by the same symmetries that describe the three Higgs doublets [7]. In such models this family symmetry could be spontaneously broken along with the EW one, with some remnant subgroup surviving, so that, for certain symmetries, it is possible to find a VEV alignment that respects the original symmetry of the (pseudo)scalar potential which will then be responsible for the stabilisation of the DM candidate [8].

One could then simply extend the I(1+1)HDM by introducing a further *inert*  $SU(2)_L$  doublet with, again, the same quantum numbers as the SM Higgs one, thereby realising a I(2+1)HDM, hence achieving the vacuum alignment  $(v, 0, 0)$ , which is of particular interest because of its I(1+1)HDM similarity and the absence of Flavour Changing Neutral Currents (FCNCs)<sup>3</sup>. This is the model we will be concerned with, building upon the one introduced and studied in Refs. [11]–[15]. Herein, though, the discrete

---

<sup>1</sup>The doublet that acquires a VEV is called the *active* doublet and the one with no VEV is called the *inert* (at times also *dark*) doublet.

<sup>2</sup>Incidentally, notice that scalar ( $H$ ) and pseudoscalar ( $A$ ) particles from the inert doublet in the I(1+1)HDM have opposite P-parity but, as they do not couple to fermions, the only means of disentangling them is to exploit their gauge interactions: e.g., the  $HAZ$  vertex is present while the  $HHZ$  and  $AAZ$  ones are not.

<sup>3</sup>A 3HDM with  $(0, v, v')$  vacuum alignment has been considered in [9] wherein it was termed IDM2. Using our nomenclature, this model may be referred to as the I(1+2)HDM.

symmetry structure used was again a  $Z_2$  one, like in 2HDMs, separating the two inert doublets and the active one. Again, the lightest  $Z_2$ -odd neutral (pseudo)scalar of this construct is the DM candidate.

In this paper, we study a variation of such a I(2+1)HDM, wherein we replace this  $Z_2$  symmetry with a  $Z_3$  one instead, following the example adopted in [16] for the case of a 2HDM. The motivation for this is to attempt generating a 3HDM with two DM candidates, thereby generating a two-component DM scenario. We shall in fact show that, in the case of a highly symmetric (pseudo)scalar potential, wherein all parameters related to one inert doublet are identical to those of the other, a realisation of the so-called ‘dark democracy’ of Ref. [13], this is indeed possible.

The layout of the remainder of the paper is as follows. In the next section we describe the aforementioned variation of the I(2+1)HDM with a  $Z_3$  symmetry whereas in Sect. 3 we introduce the dark democracy configuration. In the following section we discuss both theoretical and experimental constraints affecting our model. Numerical results will then follow while in the last section we will conclude.

## 2 The I(2+1)HDM (pseudo)scalar potential

In a NHDM, the generic (pseudo)scalar potential symmetric under a group  $G$  of phase rotations can be written as the sum of two parts:

$$V = V_0 + V_G, \quad (1)$$

where  $V_0$  is invariant under any phase rotation and  $V_G$  is a collection of extra terms ensuring the symmetry under the action of the group  $G$  [17].

The most general phase invariant part of a 3HDM potential has the following form:

$$\begin{aligned} V_0 = & -\mu_1^2(\phi_1^\dagger\phi_1) - \mu_2^2(\phi_2^\dagger\phi_2) - \mu_3^2(\phi_3^\dagger\phi_3) \\ & + \lambda_{11}(\phi_1^\dagger\phi_1)^2 + \lambda_{22}(\phi_2^\dagger\phi_2)^2 + \lambda_{33}(\phi_3^\dagger\phi_3)^2 \\ & + \lambda_{12}(\phi_1^\dagger\phi_1)(\phi_2^\dagger\phi_2) + \lambda_{23}(\phi_2^\dagger\phi_2)(\phi_3^\dagger\phi_3) + \lambda_{31}(\phi_3^\dagger\phi_3)(\phi_1^\dagger\phi_1) \\ & + \lambda'_{12}(\phi_1^\dagger\phi_2)(\phi_2^\dagger\phi_1) + \lambda'_{23}(\phi_2^\dagger\phi_3)(\phi_3^\dagger\phi_2) + \lambda'_{31}(\phi_3^\dagger\phi_1)(\phi_1^\dagger\phi_3), \end{aligned} \quad (2)$$

where the notation of [13] was used. The construction of the  $Z_3$ -symmetric part of the potential depends on the generator of the  $Z_3$  symmetry. As we want to study the model with two different DM candidates, in order to accomplish this, we will assign different charges to each doublet. More specifically, we assume that the Lagrangian is symmetric under the  $Z_3$  transformation given by

$$\phi_1 \rightarrow \omega\phi_1, \quad \phi_2 \rightarrow \omega^2\phi_2, \quad \phi_3 \rightarrow \phi_3, \quad (3)$$

with  $\omega$  being a complex cubic root of unity,  $\omega = e^{2\pi i/3}$ . In other words, we can write the generator of the group as follows:

$$g = \text{diag}(1, 2, 0). \quad (4)$$

With these assignments, the  $Z_3$  symmetric potential term  $V_G$  has the following form:

$$V_{Z_3} = -\mu_{12}^2(\phi_1^\dagger\phi_2) + \lambda_1(\phi_2^\dagger\phi_1)(\phi_3^\dagger\phi_1) + \lambda_2(\phi_1^\dagger\phi_2)(\phi_3^\dagger\phi_2) + \lambda_3(\phi_1^\dagger\phi_3)(\phi_2^\dagger\phi_3) + h.c. \quad (5)$$

It is worth mentioning that we are including the soft breaking term proportional to  $\mu_{12}^2$  in order to get rid of any degeneracies between the inert scalars and that, since we will not consider CP-violation in this paper, we require all parameters of the potential to be real. This  $Z_3$  potential can also be found in the literature [17].

We will identify  $\phi_3$  with the SM Higgs doublet and the  $Z_3$  charges for all other SM particles are considered to be zero. The Yukawa Lagrangian in this model is identical to the SM Yukawa Lagrangian (with additional terms for right-handed neutrinos) given by

$$\begin{aligned} \mathcal{L}_{Yuk} = & \Gamma_{mn}^u \bar{q}_{m,L} \tilde{\phi}_3 u_{n,R} + \Gamma_{mn}^d \bar{q}_{m,L} \phi_3 d_{n,R} \\ & + \Gamma_{mn}^e \bar{l}_{m,L} \phi_3 e_{n,R} + \Gamma_{mn}^\nu \bar{l}_{m,L} \tilde{\phi}_3 \nu_{n,R} + h.c. \end{aligned} \quad (6)$$

We assume the vacuum alignment  $\langle\phi_1\rangle = \langle\phi_2\rangle = 0$  and  $\langle\phi_3\rangle \neq 0$ , so that the  $Z_3$  symmetry is unbroken when EWSB occurs via the Higgs mechanism.

## 2.1 Mass eigenstates

We define the components of each doublet as

$$\phi_1 = \begin{pmatrix} H_1^+ \\ \frac{H_1^0 + iA_1^0}{\sqrt{2}} \end{pmatrix}, \quad \phi_2 = \begin{pmatrix} H_2^+ \\ \frac{H_2^0 + iA_2^0}{\sqrt{2}} \end{pmatrix}, \quad \phi_3 = \begin{pmatrix} H_3^+ \\ \frac{v + H_3^0 + iA_3^0}{\sqrt{2}} \end{pmatrix}. \quad (7)$$

The vacuum condition that the point  $(\phi_1^0, \phi_2^0, \phi_3^0) = (0, 0, \frac{v}{\sqrt{2}})$  becomes the minimum of the potential leads to the relation

$$v^2 = \frac{\mu_3^2}{\lambda_{33}}. \quad (8)$$

Expanding the potential around this vacuum point results in the mass spectrum below, where the pairs of scalar/pseudoscalar/charged base fields  $(H_{1,2}^0/A_{1,2}^0/H_{1,2}^\pm)$  from the inert doublets in Eq. (7) are rotated by:

$$R_{\theta_i} = \begin{pmatrix} \cos \theta_i & \sin \theta_i \\ -\sin \theta_i & \cos \theta_i \end{pmatrix}, \quad (9)$$

where  $\theta_i = \theta_h, \theta_a, \theta_c$  are the rotation angles for the scalar, pseudoscalar and charged mass-squared matrices, respectively. The mass spectrum of all (pseudo)scalar particles is presented below.

$$\mathbf{G}^0 : m_{G^0}^2 = 0$$

$$\mathbf{G}^\pm : m_{G^\pm}^2 = 0$$

$$\mathbf{h} : m_h^2 = 2\mu_3^2$$

$$\mathbf{H}_1 = \cos \theta_h H_1^0 + \sin \theta_h H_2^0 : m_{H_1}^2 = (-\mu_1^2 + \Lambda_1) \cos^2 \theta_h + (-\mu_2^2 + \Lambda_2) \sin^2 \theta_h - 2\Lambda_h \sin \theta_h \cos \theta_h$$

$$\mathbf{H}_2 = -\sin \theta_h H_1^0 + \cos \theta_h H_2^0 : m_{H_2}^2 = (-\mu_1^2 + \Lambda_1) \sin^2 \theta_h + (-\mu_2^2 + \Lambda_2) \cos^2 \theta_h + 2\Lambda_h \sin \theta_h \cos \theta_h$$

$$\text{where } \Lambda_1 = \frac{1}{2}(\lambda_{31} + \lambda'_{31})v^2, \quad \Lambda_2 = \frac{1}{2}(\lambda_{23} + \lambda'_{23})v^2, \quad \Lambda_h = \mu_{12}^2 - \frac{1}{2}\lambda_3 v^2,$$

$$\tan 2\theta_h = \frac{2\Lambda_h}{\mu_1^2 - \Lambda_1 - \mu_2^2 + \Lambda_2}.$$

$$\mathbf{A}_1 = \cos \theta_a A_1^0 + \sin \theta_a A_2^0 : m_{A_1}^2 = (-\mu_1^2 + \Lambda_1) \cos^2 \theta_a + (-\mu_2^2 + \Lambda_2) \sin^2 \theta_a - 2\Lambda_a \sin \theta_a \cos \theta_a$$

$$\mathbf{A}_2 = -\sin \theta_a A_1^0 + \cos \theta_a A_2^0 : m_{A_2}^2 = (-\mu_1^2 + \Lambda_1) \sin^2 \theta_a + (-\mu_2^2 + \Lambda_2) \cos^2 \theta_a + 2\Lambda_a \sin \theta_a \cos \theta_a$$

$$\text{where } \Lambda_1 = \frac{1}{2}(\lambda_{31} + \lambda'_{31})v^2, \quad \Lambda_2 = \frac{1}{2}(\lambda_{23} + \lambda'_{23})v^2, \quad \Lambda_a = \mu_{12}^2 + \frac{1}{2}\lambda_3 v^2,$$

$$\tan 2\theta_a = \frac{2\Lambda_a}{\mu_1^2 - \Lambda_1 - \mu_2^2 + \Lambda_2}.$$

$$\mathbf{H}_1^\pm = \cos \theta_c H_1^{0\pm} + \sin \theta_c H_2^{0\pm} : m_{H_1^\pm}^2 = (-\mu_1^2 + \Lambda'_1) \cos^2 \theta_c + (-\mu_2^2 + \Lambda'_2) \sin^2 \theta_c - 2\mu_{12}^2 \sin \theta_c \cos \theta_c$$

$$\mathbf{H}_2^\pm = -\sin \theta_c H_1^{0\pm} + \cos \theta_c H_2^{0\pm} : m_{H_2^\pm}^2 = (-\mu_1^2 + \Lambda'_1) \sin^2 \theta_c + (-\mu_2^2 + \Lambda'_2) \cos^2 \theta_c + 2\mu_{12}^2 \sin \theta_c \cos \theta_c$$

$$\text{where } \Lambda'_1 = \frac{1}{2}\lambda_{31}v^2, \quad \Lambda'_2 = \frac{1}{2}\lambda_{23}v^2,$$

$$\tan 2\theta_c = \frac{2\mu_{12}^2}{\mu_1^2 - \Lambda'_1 - \mu_2^2 + \Lambda'_2}.$$

It can be verified that, if  $\mu_{12} = 0$  (*i.e.*, eliminate the soft breaking term), then we will recover the degeneracy between the masses of  $H_1$  and  $A_1$  as well as between the masses of  $H_2$  and  $A_2$ . Note also that all the constraints on  $V_0$  from Ref. [13] can be assumed here.

In the analysis of DM physics, the triple couplings with inert scalars play an important role. In Table 1, the relevant triple couplings after EWSB are listed.

### 3 DM democracy limit

In order to demonstrate the possibility of a two components DM scenario in the I(2+1)HDM, we consider a simplified case. In the following, we assume these simple

Table 1: List of triple couplings with inert scalars. These couplings are given by the variational derivatives of the Lagrangian by the relevant fields.

Interaction	Coupling
$h H_1 H_1$	$-v((\lambda_{23} + \lambda'_{23})s_{\theta_h}^2 + (\lambda_{31} + \lambda'_{31})c_{\theta_h}^2 - 2\lambda_3 c_{\theta_h} s_{\theta_h})$
$h H_1 H_2$	$v((\lambda_{23} + \lambda'_{23} + \lambda_{31} + \lambda'_{31})c_{\theta_h} s_{\theta_h} - \lambda_3 c_{2\theta_c})$
$h H_2 H_2$	$-v((\lambda_{23} + \lambda'_{23})c_{\theta_h}^2 + (\lambda_{31} + \lambda'_{31})s_{\theta_h}^2 + 2\lambda_3 c_{\theta_h} s_{\theta_h})$
$h H_1^\pm H_1^\mp$	$-v(\lambda_{23}s_{\theta_c}^2 + \lambda_{31}c_{\theta_c}^2)$
$h H_1^\pm H_2^\mp$	$v(\lambda_{23} - \lambda_{31})c_{\theta_c} s_{\theta_c}$
$h H_2^\pm H_2^\mp$	$-v(\lambda_{23}c_{\theta_c}^2 + \lambda_{31}s_{\theta_c}^2)$
$A_1 A_1 H_1$	$-v(\lambda_1 c_{\theta_a} (c_{\theta_a} s_{\theta_h} - 2c_{\theta_h} s_{\theta_a}) - \lambda_2 s_{\theta_a} (s_{\theta_a} c_{\theta_h} - 2c_{\theta_a} s_{\theta_h}))$
$A_1 A_1 H_2$	$v(\lambda_1 c_{\theta_a} (c_{\theta_a} c_{\theta_h} + 2s_{\theta_a} s_{\theta_h}) + \lambda_2 s_{\theta_a} (s_{\theta_a} s_{\theta_h} + 2c_{\theta_a} c_{\theta_h}))$
$A_1 A_2 H_1$	$-v(\lambda_1 (c_{\theta_a} s_{\theta_a} s_{\theta_h} + c_{2\theta_a} c_{\theta_h}) + \lambda_2 (c_{\theta_a} s_{\theta_a} c_{\theta_h} - c_{2\theta_a} s_{\theta_h}))$
$A_1 A_2 H_2$	$v(\lambda_1 (c_{\theta_a} c_{\theta_h} s_{\theta_a} - c_{2\theta_a} s_{\theta_h}) - \lambda_2 (c_{\theta_a} s_{\theta_a} s_{\theta_h} + c_{2\theta_a} c_{\theta_h}))$
$A_2 A_2 H_1$	$-v(\lambda_1 s_{\theta_a} (s_{\theta_a} s_{\theta_h} + 2c_{\theta_a} c_{\theta_h}) - \lambda_2 c_{\theta_a} (c_{\theta_a} c_{\theta_h} + 2s_{\theta_a} s_{\theta_h}))$
$A_2 A_2 H_2$	$v(\lambda_1 s_{\theta_a} (s_{\theta_a} c_{\theta_h} - 2c_{\theta_a} s_{\theta_h}) + \lambda_2 c_{\theta_a} (c_{\theta_a} s_{\theta_h} - 2s_{\theta_a} c_{\theta_h}))$
$H_1 H_1 H_1$	$3v(\lambda_1 c_{\theta_h} - \lambda_2 s_{\theta_h})s_{\theta_h} c_{\theta_h}$
$H_1 H_1 H_2$	$-v(\lambda_1 c_{\theta_h} (1 - 3s_{\theta_h}^2) - \lambda_2 s_{\theta_h} (2 - 3s_{\theta_h}^2))$
$H_1 H_2 H_2$	$-v(\lambda_1 s_{\theta_h} (2 - 3s_{\theta_h}^2) + \lambda_2 c_{\theta_h} (1 - 3s_{\theta_h}^2))$
$H_2 H_2 H_2$	$-3v(\lambda_1 s_{\theta_h} + \lambda_2 c_{\theta_h})s_{\theta_h} c_{\theta_h}$
$H_1 H_1^\pm H_1^\mp$	$v(\lambda_1 c_{\theta_h} - \lambda_2 s_{\theta_h})s_{\theta_c} c_{\theta_c}$
$H_1 H_1^\pm H_2^\mp$	$-\frac{v}{2}(\lambda_1 c_{\theta_h} - \lambda_2 s_{\theta_h})c_{2\theta_c}$
$H_1 H_2^\pm H_2^\mp$	$-v(\lambda_1 c_{\theta_h} - \lambda_2 s_{\theta_h})s_{\theta_c} c_{\theta_c}$
$A_1 H_1^\pm H_2^\mp$	$-i\frac{v}{2}(\lambda_1 c_{\theta_a} + \lambda_2 s_{\theta_a})$

relations between the parameters associated to the two inert doublets:

$$\mu_1^2 = n\mu_2^2, \quad \lambda_{11} = n\lambda_{22}, \quad \lambda_{31} = n\lambda_{23}, \quad \lambda'_{31} = n\lambda'_{23}, \quad \lambda_1 = n\lambda_2, \quad (10)$$

that lead to

$$\Lambda_1 = n\Lambda_2, \quad \Lambda'_1 = n\Lambda'_2. \quad (11)$$

With this ansatz, the mass eigenvalues are also simplified to

$$\begin{aligned} m_{H_1}^2 &= (-\mu_2^2 + \Lambda_2)(n \cos^2 \theta_h + \sin^2 \theta_h) - 2\Lambda_h \sin \theta_h \cos \theta_h, \\ m_{H_2}^2 &= (-\mu_2^2 + \Lambda_2)(n \sin^2 \theta_h + \cos^2 \theta_h) + 2\Lambda_h \sin \theta_h \cos \theta_h, \end{aligned} \quad (12)$$

Table 2: List of three scalar couplings with inert scalars in the case where all parameters in the dark scalar sector are proportional (see Eq. (10)). These couplings are given by the variational derivative of the Lagrangian by the relevant fields.

Interaction	Coupling
$h H_1 H_1$	$-v((\lambda_{23} + \lambda'_{23})(s_{\theta_h}^2 + nc_{\theta_h}^2) - 2\lambda_3 c_{\theta_h} s_{\theta_h})$
$h H_1 H_2$	$v((\lambda_{23} + \lambda'_{23})(1 - n)c_{\theta_h} s_{\theta_h} - \lambda_3 c_{2\theta_h})$
$h H_2 H_2$	$-v((\lambda_{23} + \lambda'_{23})(ns_{\theta_h}^2 + c_{\theta_h}^2) + 2\lambda_3 c_{\theta_h} s_{\theta_h})$
$h H_1^\pm H_1^\mp$	$-v\lambda_{23}(s_{\theta_c}^2 + nc_{\theta_c}^2)$
$h H_1^\pm H_2^\mp$	$v\lambda_{23}(1 - n)c_{\theta_c} s_{\theta_c}$
$h H_2^\pm H_2^\mp$	$-v\lambda_{23}(c_{\theta_c}^2 + ns_{\theta_c}^2)$
$A_1 A_1 H_1$	$-v\lambda_2(nc_{\theta_a}(c_{\theta_a} s_{\theta_h} - 2c_{\theta_h} s_{\theta_a}) - s_{\theta_a}(s_{\theta_a} c_{\theta_h} - 2c_{\theta_a} s_{\theta_c}))$
$A_1 A_1 H_2$	$v\lambda_2(nc_{\theta_a}(c_{\theta_a} c_{\theta_h} + 2s_{\theta_a} s_{\theta_h}) + s_{\theta_a}(s_{\theta_a} s_{\theta_h} + 2c_{\theta_a} c_{\theta_h}))$
$A_1 A_2 H_1$	$-v\lambda_2(n(c_{\theta_a} s_{\theta_a} s_{\theta_h} + c_{2\theta_a} c_{\theta_h}) + (c_{\theta_a} s_{\theta_a} c_{\theta_h} - c_{2\theta_a} s_{\theta_h}))$
$A_1 A_2 H_2$	$v\lambda_2(n(c_{\theta_a} c_{\theta_h} s_{\theta_a} - c_{2\theta_a} s_{\theta_h}) - (c_{\theta_a} s_{\theta_a} s_{\theta_h} + c_{2\theta_a} c_{\theta_h}))$
$A_2 A_2 H_1$	$-v\lambda_2(ns_{\theta_a}(s_{\theta_a} s_{\theta_h} + 2c_{\theta_a} c_{\theta_h}) - c_{\theta_a}(c_{\theta_a} c_{\theta_h} + 2s_{\theta_a} s_{\theta_h}))$
$A_2 A_2 H_2$	$v\lambda_2(ns_{\theta_a}(s_{\theta_a} c_{\theta_h} - 2c_{\theta_h} s_{\theta_a}) + c_{\theta_a}(c_{\theta_a} s_{\theta_h} - 2s_{\theta_a} c_{\theta_h}))$
$H_1 H_1 H_1$	$3v\lambda_2(nc_{\theta_h} - s_{\theta_h})s_{\theta_h} c_{\theta_h}$
$H_1 H_1 H_2$	$-v\lambda_2(nc_{\theta_h}(1 - 3s_{\theta_h}^2) - s_{\theta_h}(2 - 3s_{\theta_h}^2))$
$H_1 H_2 H_2$	$-v\lambda_2(ns_{\theta_h}(2 - 3s_{\theta_h}^2) + c_{\theta_h}(1 - 3s_{\theta_h}^2))$
$H_2 H_2 H_2$	$-3v\lambda_2(ns_{\theta_h} + c_{\theta_h})s_{\theta_h} c_{\theta_h}$

and the mixing angle for the CP-even inert scalars is given by

$$\tan 2\theta = \frac{-2\Lambda_h}{(n-1)(-\mu_2^2 + \Lambda_2)}. \quad (13)$$

The formulae for the mass eigenvalues and the mixing angles of the CP-odd scalars and of the charged scalars are given by the replacement of the parameters  $(\Lambda_h, \Lambda_2, \theta_h) \rightarrow (\Lambda_a, \Lambda'_2, \theta_a)$  and  $(\Lambda_h, \Lambda_2, \theta_h) \rightarrow (\mu_{12}^2, \Lambda'_2, \theta_c)$ , respectively. The triple couplings with inert scalars in this simplified case are listed in Table 2.

As a benchmark scenario, we focus on the particular case with  $n = 1$  that corresponds to the so-called dark democracy limit [13]. This limit imposes a new  $Z_3$  symmetry ( $Z'_3$  on the Lagrangian, namely the model is  $Z_3 \times Z'_3$  invariant). Under the  $Z'_3$ , the three doublets are rotated as

$$\phi_1 \rightarrow \omega \phi_2, \quad \phi_2 \rightarrow \omega^2 \phi_1, \quad \phi_3 \rightarrow \phi_3. \quad (14)$$

Table 3: The triple couplings with inert scalars in the dark democracy limit are listed. These couplings are given by the variational derivative of the Lagrangian by the relevant fields.

Interaction	Coupling	Interaction	Coupling
$h H_1 H_1$	$-v(\lambda_{23} + \lambda'_{23} - \lambda_3)$	$H_1 H_1 H_1$	0
$h H_1 H_2$	0	$H_1 H_1 H_2$	$\frac{1}{\sqrt{2}}v\lambda_2$
$h H_2 H_2$	$-v(\lambda_{23} + \lambda'_{23} + \lambda_3)$	$H_1 H_2 H_2$	0
$h H_{1,2}^\pm H_{1,2}^\pm$	$-v\lambda_{23}$	$H_2 H_2 H_2$	$-\frac{3}{\sqrt{2}}v\lambda_2$
$A_1 A_1 H_1$	0	$H_1 H_{1,2}^\pm H_{1,2}^\mp$	0
$A_1 A_1 H_2$	$\frac{3}{\sqrt{2}}v\lambda_2$	$H_2 H_1^\pm H_1^\mp$	$\pm\frac{v}{\sqrt{2}}\lambda_2$
$A_1 A_2 H_1$	$-\frac{1}{\sqrt{2}}v\lambda_2$	$A_1 H_{1,2}^\pm H_{2,1}^\mp$	$\mp i\frac{v}{\sqrt{2}}\lambda_2$
$A_1 A_2 H_2$	0	$A_2 H_1^\pm H_2^\mp$	0
$A_2 A_2 H_1$	0		
$A_2 A_2 H_2$	$-\frac{1}{\sqrt{2}}v\lambda_2$		

(Similarly to the SM Higgs doublet  $\phi_3$ , all the other SM particles are considered to be charge zero also under the  $Z'_3$  symmetry.) The triple couplings with inert (pseudo)scalars in this limit are listed in Table 3.

In this dark democracy limit, the mass terms of the inert doublets are simplified to

$$\mathcal{L}_m = -\frac{1}{2}(M_H^2)_{ij}H_i^0H_j^0 - \frac{1}{2}(M_A^2)_{ij}A_i^0A_j^0 - (M_{H^\pm}^2)_{ij}H_i^+H_j^-, \quad (15)$$

with

$$\begin{aligned} (M_H^2) &= \begin{pmatrix} -\mu_2^2 + \Lambda_2 & -\Lambda_h \\ -\Lambda_h & -\mu_2^2 + \Lambda_2 \end{pmatrix}, & (M_A^2) &= \begin{pmatrix} -\mu_2^2 + \Lambda'_2 & -\Lambda_a \\ -\Lambda_a & -\mu_2^2 + \Lambda'_2 \end{pmatrix}, \\ (M_{H^\pm}^2) &= \begin{pmatrix} -\mu_2^2 + \Lambda'_2 & -\mu_{12}^2 \\ -\mu_{12}^2 & -\mu_2^2 + \Lambda'_2 \end{pmatrix}. \end{aligned} \quad (16)$$

Then we can diagonalise all the three mass matrices  $M_\phi^2(\phi = H, A, H^\pm)$  by the matrix  $R_{\pi/4}$  as

$$R_{\pi/4}(M_\phi^2)R_{\pi/4}^T = \begin{pmatrix} (M_\phi^2)_{11} + (M_\phi^2)_{12} & 0 \\ 0 & (M_\phi^2)_{11} - (M_\phi^2)_{12} \end{pmatrix} \quad (\phi = H, A, H^\pm), \quad (17)$$

which leads to  $\theta_h = \theta_a = \theta_c = \frac{\pi}{4}$ . Then the eigenvalues are given by

$$\begin{aligned}
m_{H_1}^2 &= \frac{1}{2}v^2(\lambda_{23} + \lambda'_{23} + \lambda_3) - \mu_{12}^2 - \mu_2^2, \\
m_{A_1}^2 &= \frac{1}{2}v^2(\lambda_{23} + \lambda'_{23} - \lambda_3) - \mu_{12}^2 - \mu_2^2, \\
m_{H_2}^2 &= \frac{1}{2}v^2(\lambda_{23} + \lambda'_{23} - \lambda_3) + \mu_{12}^2 - \mu_2^2, \\
m_{A_2}^2 &= \frac{1}{2}v^2(\lambda_{23} + \lambda'_{23} + \lambda_3) + \mu_{12}^2 - \mu_2^2, \\
m_{H_1^\pm}^2 &= \frac{1}{2}v^2\lambda_{23} - \mu_{12}^2 - \mu_2^2, \\
m_{H_2^\pm}^2 &= \frac{1}{2}v^2\lambda_{23} + \mu_{12}^2 - \mu_2^2.
\end{aligned} \tag{18}$$

Note that in the dark democracy limit the two DM candidates always have opposite CP charge. This can be seen explicitly from using mass formulae in Eq. (18) to get the mass relations as

$$\begin{aligned}
m_{A_1}^2 &= m_{H_2}^2 - m_{H_2^\pm}^2 + m_{H_1^\pm}^2, \\
m_{A_2}^2 &= m_{H_1}^2 + m_{H_2^\pm}^2 - m_{H_1^\pm}^2.
\end{aligned} \tag{19}$$

Then, if  $H_{1(2)}$  is the lightest inert scalar, the second lightest is  $A_{1(2)}$  and, if  $A_{1(2)}$  is the lightest, the second lightest is  $H_{1(2)}$ .

We can rewrite the Lagrangian parameters  $\mu_2^2$ ,  $\mu_{12}^2$ ,  $\lambda_{23}$ ,  $\lambda'_{23}$  and  $\lambda_3$  by using the mass eigenvalues and a dimensionless parameter  $g_{\text{DM}} = \lambda_{23} + \lambda'_{23} - \lambda_3$  as

$$\begin{aligned}
\mu_2^2 &= -m_{H_2}^2 + \frac{\Delta_+}{2} + \frac{v^2}{2}g_{\text{DM}}, \quad \mu_{12}^2 = \frac{\Delta_+}{2}, \\
\lambda_{23} &= \frac{2\Delta_2}{v^2} + g_{\text{DM}}, \quad \lambda'_{23} = -\frac{\Delta_1 + \Delta_2}{v^2}, \quad \lambda_3 = \frac{\Delta_2 - \Delta_1}{v^2},
\end{aligned} \tag{20}$$

where  $\Delta_1$ ,  $\Delta_2$  and  $\Delta_+$  are the mass squared differences given by

$$\Delta_1 = m_{H_1^\pm}^2 - m_{H_1}^2, \quad \Delta_2 = m_{H_2^\pm}^2 - m_{H_2}^2, \quad \Delta_+ = m_{H_2^\pm}^2 - m_{H_1^\pm}^2. \tag{21}$$

In our analysis, we use the following five free parameters:

$$m_{H_1}, m_{H_2}, m_{H_1^\pm}, m_{H_2^\pm}, g_{\text{DM}}.$$

Let us comment on our convention for the mixing angle  $\theta_h = \theta_a = \theta_c = \pi/4$ . In the DM democracy limit, one can also diagonalise each of the mass matrices ( $M_\phi^2$ ) by using  $R_{-\pi/4}$  instead of  $R_{\pi/4}$  as

$$R_{-\pi/4}(M_\phi^2)R_{-\pi/4}^T = \begin{pmatrix} (M_\phi^2)_{11} - (M_\phi^2)_{12} & 0 \\ 0 & (M_\phi^2)_{11} + (M_\phi^2)_{12} \end{pmatrix} \quad (\phi = H, A, H^\pm). \quad (22)$$

With this diagonalisation, the labels of mass eigenstates are exchanged compared to our convention. For example, when one take  $\theta_h = -\pi/4$  instead of  $\theta_h = \pi/4$ , it causes the exchange of  $H_1 \leftrightarrow H_2$  in the mass eigenvalues and couplings. It does not cause any physical effect on the DM physics but just a conventional relabeling.

## 4 Constraints on parameters

As the third doublet is identified with the SM Higgs doublet,  $\mu_3, \lambda_{33}$  are Higgs field parameters, renormalised by the Higgs mass. We use the value  $m_h = 125$  GeV for the latter, so that

$$m_h^2 = 2\mu_3^2 = 2\lambda_{33}v^2. \quad (23)$$

For the  $V_0$  part of the potential to have a stable vacuum (bounded from below), the following conditions are required [12]:

- $\lambda_{11}, \lambda_{22}, \lambda_{33} > 0$  (24)
- $\lambda_{12} + \lambda'_{12} > -2\sqrt{\lambda_{11}\lambda_{22}}$
- $\lambda_{23} + \lambda'_{23} > -2\sqrt{\lambda_{22}\lambda_{33}}$
- $\lambda_{31} + \lambda'_{31} > -2\sqrt{\lambda_{33}\lambda_{11}}$

We also require the parameters of the  $V_{Z_3}$  part to be smaller than the parameters of the  $V_0$  part:

- $|\lambda_2|, |\lambda_3| < |\lambda_{ii}|, |\lambda_{ij}|, |\lambda'_{ij}|, \quad i \neq j = 1, 2, 3$  (25)

For the point  $(0, 0, \frac{v}{\sqrt{2}})$  to be a minimum of the potential, the second order derivative matrix must have positive definite determinant. Therefore, it is required that:

$$\bullet \quad \left( -\mu_2^2 + (\lambda_{23} + \lambda'_{23})\frac{v^2}{2} \right)^2 > |\mu_{12}^2|^2 \quad (26)$$

Measurements done at LEP limit the invisible decays of  $Z$  and  $W^\pm$  gauge bosons, requiring that [22, 23]

- $m_{H_i^\pm} + m_{H_i, A_i} > m_{W^\pm}$  (27)
- $m_{H_i} + m_{A_i} > m_Z$
- $2m_{H_i^\pm} > m_Z$

Also, LEP provides a model-independent lower limit for the mass of the charged scalars:

- $m_{H_i^\pm} > 70 - 90$  GeV. (28)

Searches for charginos and neutralinos at LEP have been translated into limits of region of masses in the I(1+1)HDM [23] where for

$$m_H < 80 \text{ GeV} \quad \text{and} \quad m_A < 100 \text{ GeV}$$

the following region is excluded

- $m_A - m_H > 8$  GeV. (29)

We have taken this limit into account in our numerical studies for any pair of CP-even and CP-odd particles.

A scan over some parameter space can be seen in Figure 1. In here we are scanning:

- $60 \text{ GeV} < m_{H_1}, m_{H_2} < 110 \text{ GeV}$
- $100 \text{ GeV} < m_{H_1^\pm}, m_{H_2^\pm} < 150 \text{ GeV}$
- $-1.5 < g_{\text{DM}} < 1.5$

Finally, the decay width of the Higgs decaying into a pair of the inert scalars is:

$$\Gamma(h \rightarrow SS) = \frac{\lambda^2 v^2}{32\pi m_h} \sqrt{1 - \frac{4m_S^2}{m_h^2}}, \quad (30)$$

with  $S = H_1, H_2, A_1, A_2$  if  $m_S < m_h/2$ , where  $m_S$  is the mass of the corresponding neutral inert particle and  $\lambda$  its coupling to the SM Higgs boson. Experimental measurements of invisible Higgs decays limit models in which the Higgs boson can decay into lighter particles which escape detection. The current limits on the SM-like Higgs boson invisible (inv) Branching Ratio (BR) from the ATLAS and CMS experiments are [24, 25]

$$\text{BR}(h \rightarrow \text{inv}) < 0.23 - 0.36. \quad (31)$$

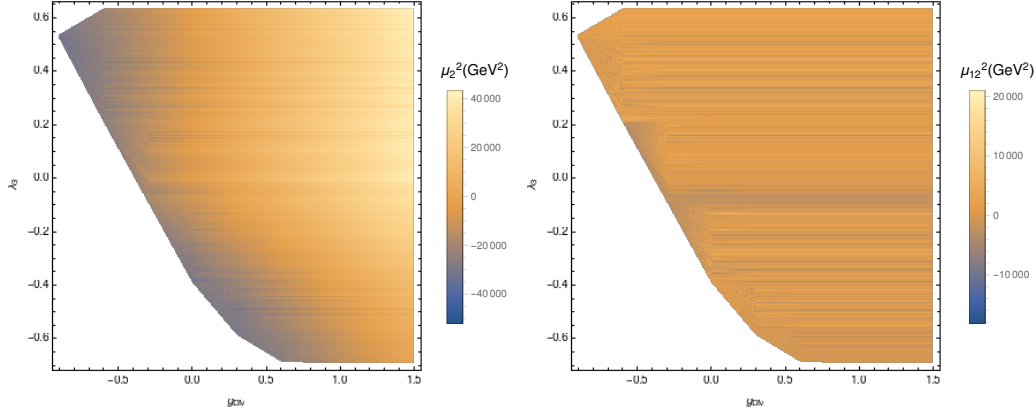


Figure 1: Parameter space compatible with all the theoretical and experimental constraints mentioned. First plot shows the dependence between the parameters  $(\lambda_3, g_{\text{DM}})$  and  $\mu_2^2$ . Second plot shows the dependence between the parameters  $(\lambda_3, g_{\text{DM}})$  and  $\mu_{12}^2$ .

This limit leads to strong constraints on the  $H_1 H_1 h$  coupling (roughly  $\lambda \lesssim 0.02$  for masses  $m_{H_1} \lesssim m_h/2$ ).

For our scenarios this BR is:

$$\text{BR}(h \rightarrow \text{inv}) = \frac{\Sigma_{i,j} \Gamma(h \rightarrow S_i S_j)}{\Gamma_h^{\text{SM}} + \Sigma_{i,j} \Gamma(h \rightarrow S_i S_j)}, \quad (32)$$

where  $S_i S_j = A_1 H_2$  or  $H_2 A_1$ .

## 5 Results

### 5.1 Relic density

First, we consider the relic abundance of DM. As a reference value, we use the one measured by Planck [19]:

$$\Omega_{\text{DM}} h^2 = 0.1198 \pm 0.0027, \quad (33)$$

and we present benchmark scenarios in which this observed quantity is reproduced, *i.e.*, the two components of DM in the  $Z_3$  symmetric I(2+1)HDM saturate the above value. In particular, due to the presence of two DM candidates in this model, the prediction of the total relic density is given by  $\Omega_{\text{DM}} h^2 = \Omega_{\text{DM-1}} h^2 + \Omega_{\text{DM-2}} h^2$ . In the following, we present the relic density obtained in different scenarios. For the numerical evaluation of the relic abundance, we use micrOMEGAs [18].

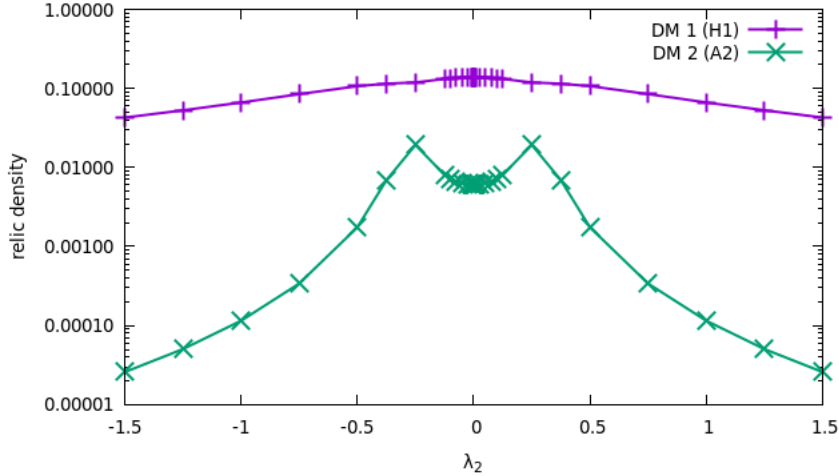


Figure 2: This plot shows the effect of  $\lambda_2$  (via DM semi-annihilation) on the relic density. Here,  $m_{H_1} = 76$  GeV,  $m_{H_2} = 98$  GeV,  $m_{H_1^\pm} = 110$  GeV,  $m_{H_2^\pm} = 112$  GeV,  $\lambda_{11} = \lambda_{22} = \lambda_{12} = \lambda'_{12} = 0.3$  and  $g_{\text{DM}} = -0.001$ . Note that the contribution of the two DM candidates is comparable within the region  $-0.25 \leq \lambda_2 \leq 0.25$ .

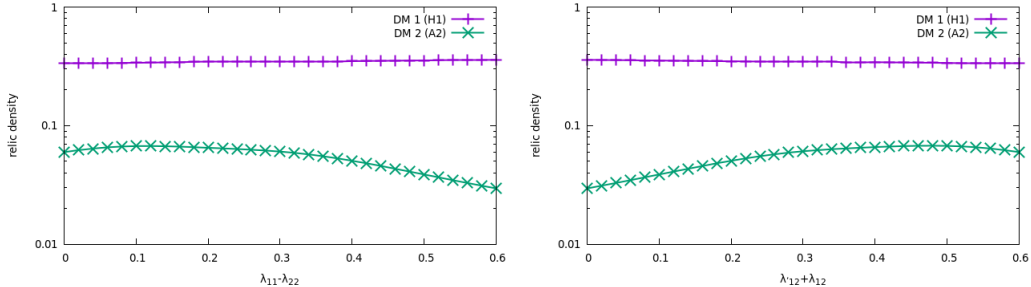


Figure 3: The first plot shows the effect of  $\lambda_{11} - \lambda_{22}$  (via partial DM conversion) and the second that of  $\lambda_{12} + \lambda'_{12}$  (via total DM conversion) on the relic density. Here,  $m_{H_1} = 74$  GeV,  $m_{H_2} = 96$  GeV,  $m_{H_1^\pm} = 108$  GeV,  $m_{H_2^\pm} = 110$  GeV,  $\lambda_2 = -0.25$  and  $g_{\text{DM}} = -0.001$ . Neither of these scenarios is actually viable.

Differently from the one DM component case, in our scenario with two DM components (here generically labelled as  $S_i$  with  $i = 1, 2$  and  $S = A, H$ ), the following three additional processes (wherein  $m_{S_2} > m_{S_1}$ ) can affect the DM relic abundance of the two DM sectors.

- DM semi-annihilation:  $S_2 S_2 \rightarrow h S_1$  where  $S = H, A$ . The vertices are proportional to  $\lambda_2$ . The plot in Figure 2 shows the effect of  $\lambda_2$  on the relic density.
- Partial DM conversion:  $S_2 S_2 \rightarrow S_2 S_1$  where  $S = H, A$ . The vertices are proportional to  $\lambda_{11} - \lambda_{22}$ . The plot on the left of Figure 3 shows the effect of  $\lambda_{11} - \lambda_{22}$  on the relic density.
- Total DM conversion:  $S_2 S_2 \rightarrow S_1 S_1$  where  $S = H, A$ . The vertices are proportional to  $(\lambda_{11} + \lambda_{22})$  and  $(\lambda_{12} + \lambda'_{12})$ . The plot on the right of Figure 3 shows the effect of  $\lambda_{12} + \lambda'_{12}$  on the relic density.

According to Figures 2–3, it is clear that only the first of the three mechanisms above is phenomenologically acceptable. Further, we need to pick a value of  $\lambda_2$  in the interval  $-0.25 \leq \lambda_2 \leq 0.25$  if we want to find a scenario for which the observed relic density is reproduced with the two DM components being of comparable magnitude. Herein and in the following, we fix the rest of coupling parameters  $\lambda_{ij}$  to be 0.3 while the inert masses have representative values.

In the following, we analyse the relic abundance in several scenarios, each of the latter being characterised by different mass differences of the inert (pseudo)scalars, the latter being the driving kinematical parameters affecting  $\Omega_{\text{DM-1}} h^2 + \Omega_{\text{DM-2}} h^2$ .

- **Non-degenerate scenario**

In this configuration, we fix

$$m_{H_2} - m_{H_1} = 17 \text{ GeV}, \quad m_{H_2^\pm} - m_{H_2} = 9 \text{ GeV}, \quad m_{H_1^\pm} - m_{H_1} = 36 \text{ GeV}, \quad (34)$$

with the value of the CP-even, CP-odd and charged inert masses allowed random relative values. In Figure 4, we show the relic density as a function of the parameters  $g_{\text{DM}}$  and  $\lambda_2$ . The DM candidates in this scenario are  $H_1$  and  $A_2$ , the latter being the lightest. In this scenario, the relic abundance of the heavier DM candidate is much smaller than the observed one. The abundance of the lighter DM candidate shows a similar dependence on the mass to the case of the IDM.

- **Charged degeneracy**

In this scenario, we fix

$$m_{H_2} - m_{H_1} = 22 \text{ GeV}, \quad m_{H_2^\pm} - m_{H_2} = 12 \text{ GeV}, \quad m_{H_1^\pm} - m_{H_1} = 34 \text{ GeV}. \quad (35)$$

Note that here  $m_{H_1}^\pm = m_{H_2}^\pm$  and hence the DM candidates,  $H_1$  and  $A_2$ , also have equal masses (from Eq. (19)), see Figure 5. In this scenario, we can reproduce the measured value of the relic density both in the low mass region ( $m_{\text{DM}} < m_h/2$ ) and in the medium mass region ( $m_h/2 < m_{\text{DM}} < m_{W^\pm}$ ). But for larger DM masses, it is under-produced. To get the proper value of relic density, the value of  $g_{\text{DM}}$  is tuned. The dependence of the abundance on the parameter  $g_{\text{DM}}$  is shown in Figure 6, where it can be noted that, for a mass of  $m_{H_1} = m_{A_2} = 64$  GeV, the proper value is  $g_{\text{DM}} \approx 0.035$ .

- **CP-even degeneracy**<sup>4</sup>

In this scenario, we fix

$$m_{H_1} - m_{H_2} = 0, \quad m_{H_2^\pm} - m_{H_2} = 46 \text{ GeV}, \quad m_{H_1^\pm} - m_{H_1} = 16 \text{ GeV}. \quad (36)$$

The DM candidates are  $A_1$  and  $H_2$ . The difference in mass between these two decreases for larger masses of  $H_2$ , see Figure 7. Note that the lightest DM candidate shows a behaviour very similar to that of the IDM, except that the value of the relic density is much lower. The heavier DM candidate is not really contributing to the total relic density.

- **Heavy DM**

In this scenario, we explored the relic density obtained for heavier masses of the inert scalars. We fix

$$m_{H_2} - m_{H_1} = 30 \text{ GeV}, \quad m_{H_2^\pm} - m_{H_2} = 90 \text{ GeV}, \quad m_{H_1^\pm} - m_{H_1} = 90 \text{ GeV}. \quad (37)$$

The DM candidates are  $H_2$  and  $A_1$ , see Figure 8. Note that in the heavy mass region, the relic density is always under-produced.

As it can be observed, of the possible scenarios described, the more interesting one is the case of charged degeneracy, since for this scenario not only can we reproduce the observed value of the relic density, but also the two DM candidates are contributing equally to it. By raising this degeneracy slightly, the heavy DM candidate contributes less to the relic density depending on the difference between the masses, as can be seen in Figure 9. Figure 10 finally shows the dependence on  $g_{\text{DM}}$  for mass splittings of 1, 3 and 8 GeV, respectively.

---

<sup>4</sup>The case of CP-odd degeneracy is not dissimilar, with the role of the neutral inert states being inverted.

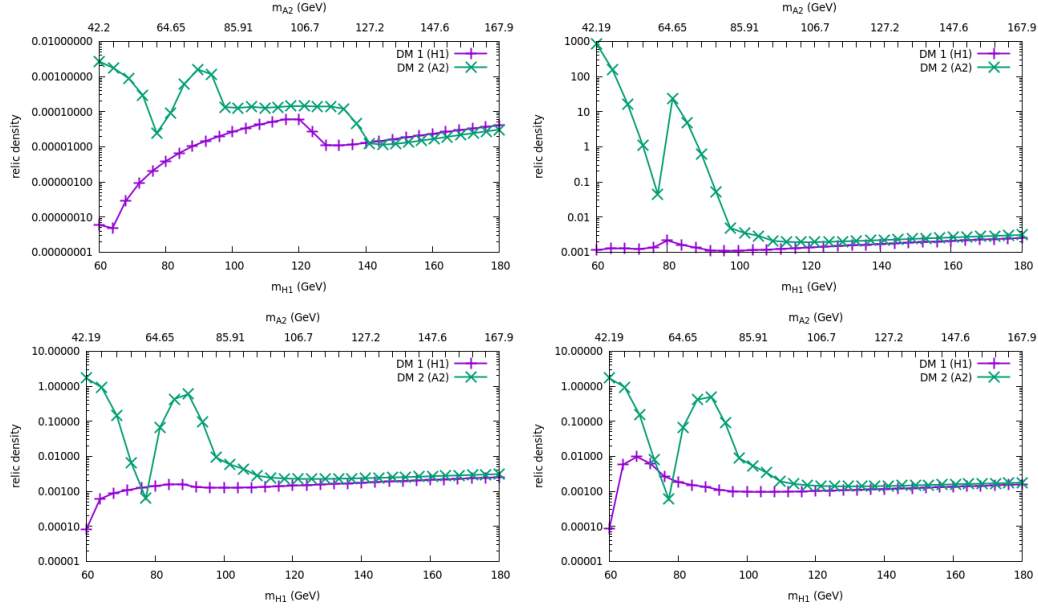


Figure 4: Relic density in the non-degenerate scenario. In the two plots on the top  $\lambda_2 = 0.0001$  with  $g_{\text{DM}} = -1.5$  on the right and  $g_{\text{DM}} = -0.001$  on the left. In the plots at the bottom  $g_{\text{DM}} = -0.05$  with  $\lambda_2 = 0.0001$  on the left and  $\lambda_2 = -0.25$  on the right. It can be observed that the DM candidate  $H_1$  almost does not contribute to the total relic density while the DM candidate  $A_2$  has a behaviour similar to the IDM.

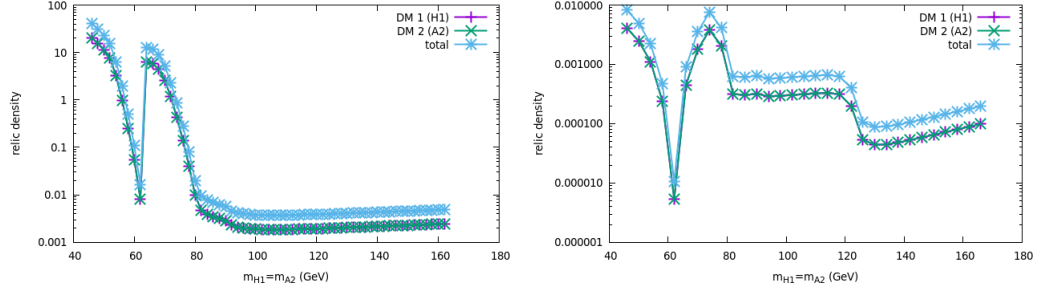


Figure 5: Relic density in the charged degeneracy scenario. In these plots we show the relic density abundance for  $g_{\text{DM}} = -0.001$  and  $g_{\text{DM}} = -1.0$ , where mass splittings are fixed as in Eq. (35) and  $\lambda_2 = -0.25$ . In this scenario the masses of the two charged inerts are degenerate and consequently, the two DM candidates are also degenerate. Note that for this scenario the two DM candidates are contributing equally to the total relic density.

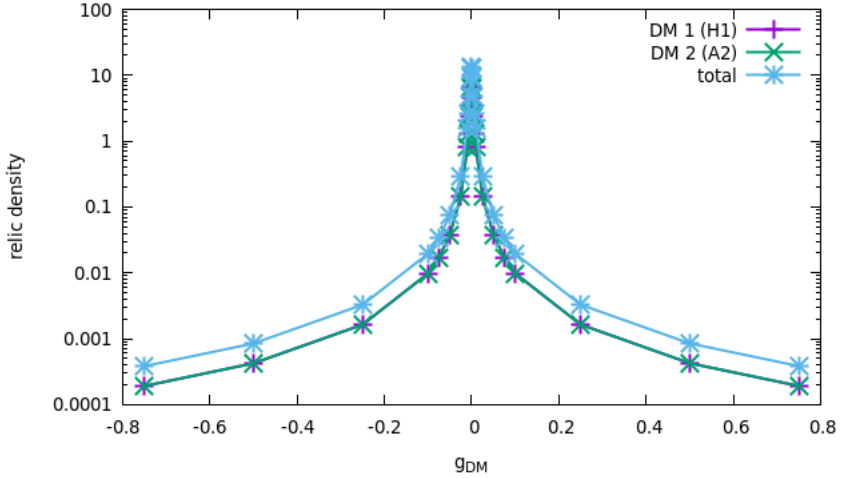


Figure 6: Relic density in the charged degeneracy scenario. Dependence of the relic density on the parameter  $g_{\text{DM}}$ . In this plot  $m_{H_1} = m_{A_2} = 64$  GeV,  $m_{H_2} = m_{A_1} = 86$  GeV and  $m_{H_{1,2}^\pm} = 98$  GeV. The proper relic density for this case can be obtained when  $g_{\text{DM}} \approx \pm 0.03$ .

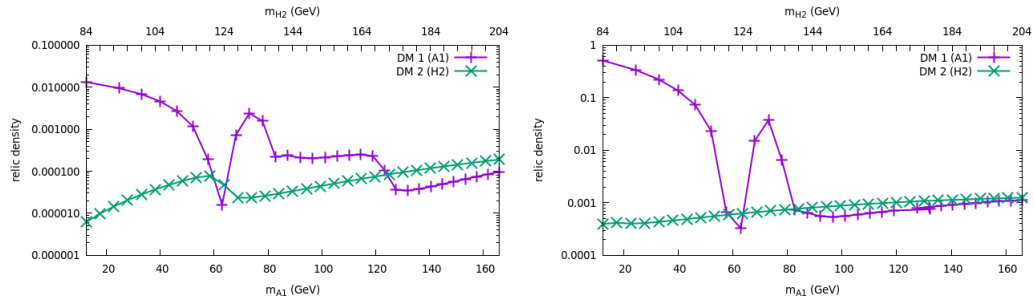


Figure 7: Relic density in the CP-even degeneracy scenario. In these plots we show the relic density abundance for two different values of  $g_{\text{DM}} = -1.5, -0.05$ . Similarly to the case of the non-degenerate scenario, the heavier DM candidate ( $H_2$  in this case) contributes very little to the total relic density.

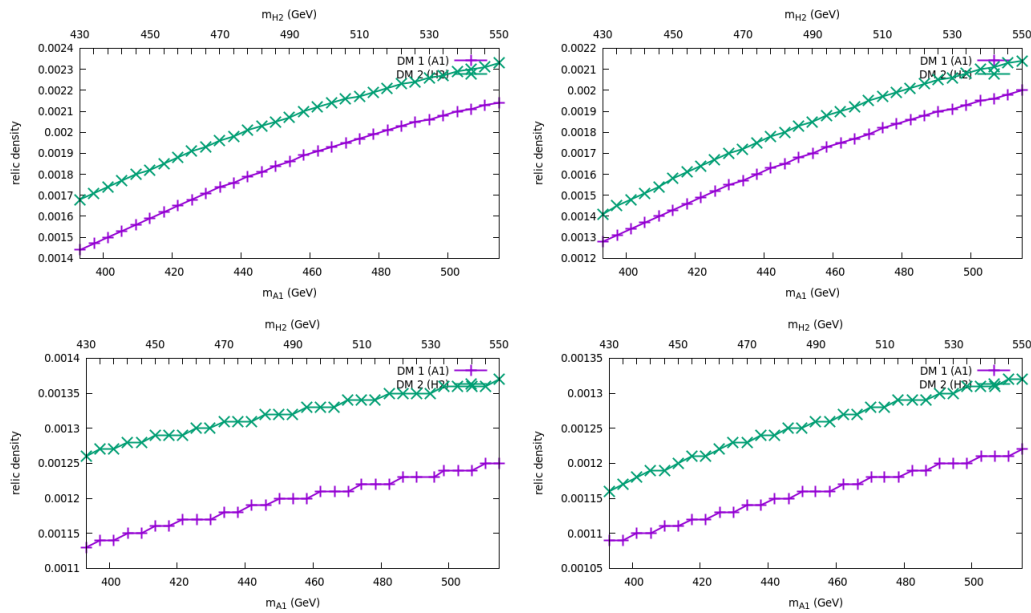


Figure 8: Relic density in the heavy DM scenario. In the plots at the top  $g_{\text{DM}} = -1.5$  while in the plots at the bottom  $g_{\text{DM}} = -0.001$  with  $\lambda_2 = 0.0001$  for the plots on the left and  $\lambda_2 = -0.25$  for the plots on the right. The relic density for any DM above 100 GeV is always under-produced.

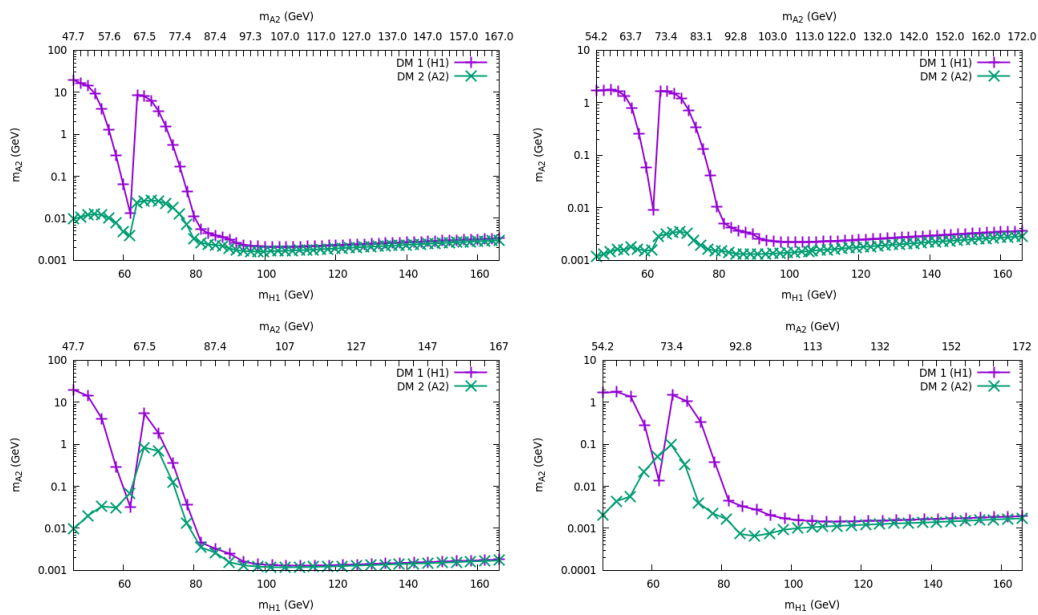


Figure 9: In these plots we show the relic density for a scenario where the mass difference between the two charged inerts is 1 GeV (left) and 5 GeV (right). In the upper plots  $\lambda_2 = 0.0001$  and in the lower plots  $\lambda_2 = -0.25$ . It can be noted how semi-annihilation processes affect the relic density of  $A_2$  particles.

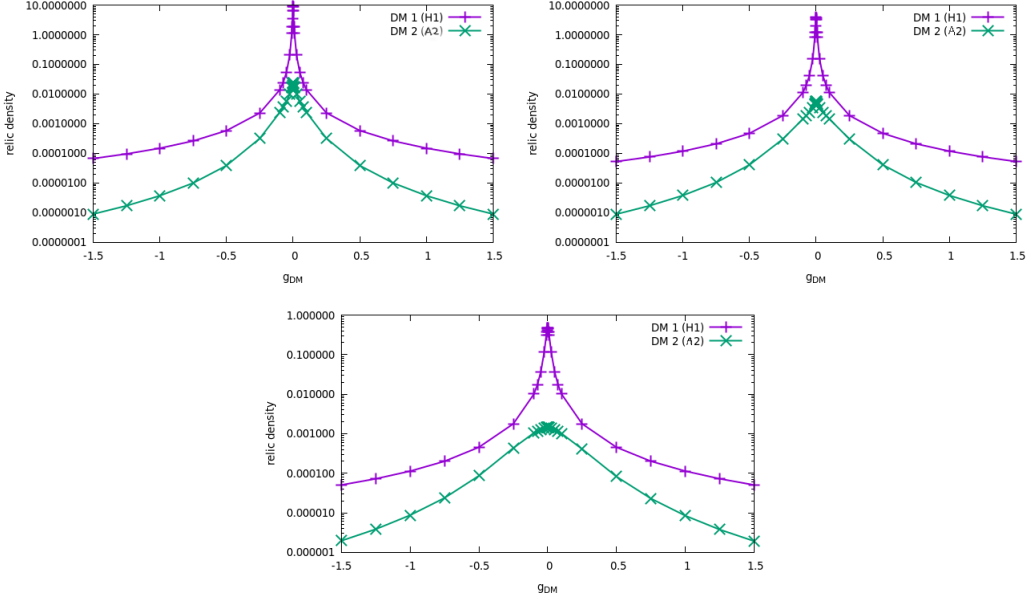


Figure 10: In these plots we show the relic density dependence when we change the mass difference of the charged masses. The mass difference is 1 GeV in the first, 3 GeV in the second and 8 GeV in the third (clock-wise).

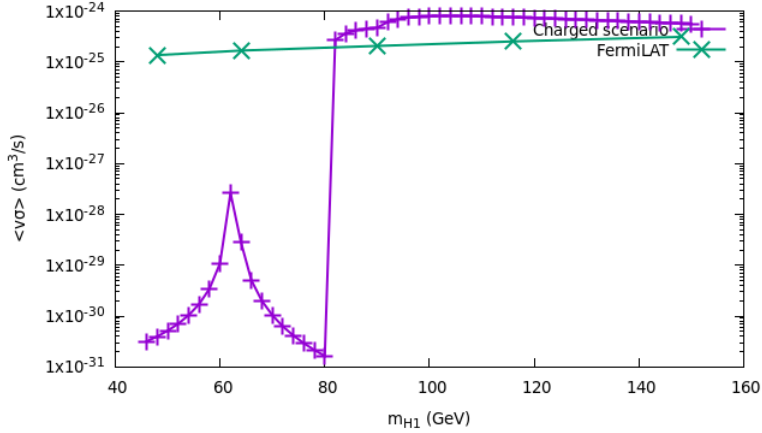


Figure 11: The charged degeneracy scenario against the indirect detection cross section limits from FermiLAT. Only the mass region below 80 GeV is in accordance with the results from Ref. [33].

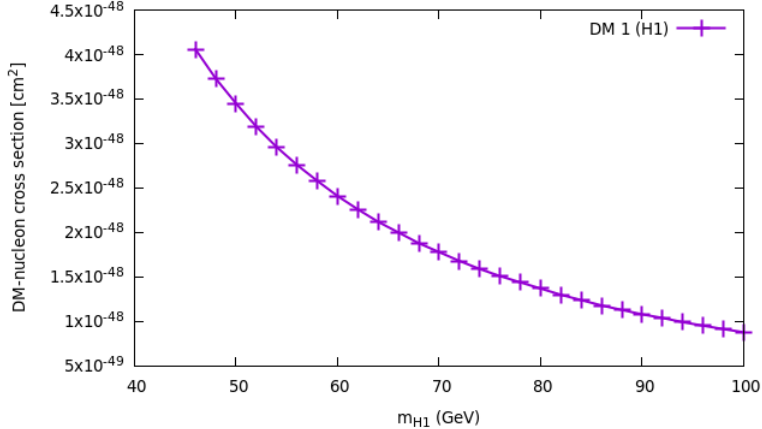


Figure 12: In this plot we show the DM-nucleon cross section for the scenario where the charged mass difference is 5 GeV and  $g_{\text{DM}} = -0.001$ . As this plot shows, this scenario is in accordance with the results from LUX [31] and Xenon1T [31].

In addition, the parameters analysed in the charged degeneracy scenario are compatible with the observations of FermiLAT (see Figure 11) and with the observations of LUX and Xenon1T (see Figure 12). To calculate the direct detection (spin-independent) cross section we used the following expression from Ref. [26]:

$$\sigma(\phi N \rightarrow \phi N) = \frac{c_S^2}{4m_h^4} \frac{m_N^2}{\pi(m_S + m_N)^2} f_N^2, \quad (38)$$

where  $\phi$  is the DM candidate,  $c_S$  is the coupling with the (pseudo)scalar state and  $N$  represents a nucleon (proton or neutron) with its mass  $m_N \simeq 1$  GeV. The parameter  $f_N$  depends on hadronic matrix elements as

$$f_N = \Sigma_q m_q \langle N | \bar{q}q | N \rangle - \frac{\alpha_s}{4\pi} \langle G_{\mu\nu} G^{\mu\nu} | n \rangle \quad (39)$$

$$= \Sigma_q m_N f_{Tq} + \frac{2}{9} m_N f_{TG}. \quad (40)$$

According to Ref. [26], we can take  $f_{Tu} + f_{Td} \simeq 0.056$ ,  $f_{Ts} = 0$  (in a conservative analysis) and  $1 = f_{Tu} + f_{Td} + f_{Ts} + f_{TG}$ .

## 5.2 Other experimental constraints

Constraints on the model come from such processes as those described in Section 4, *i.e.*, contribution to the width of gauge bosons, search for charged scalars, IDM or Mini-

mal Supersymmetric Standard Model (MSSM) at LEP and the Higgs invisible decays. However, having learnt the relevance of the charged inert sector, we emphasise here that there are additional constraints that must be satisfied, wherein  $H_{1,2}^\pm$  states play a crucial role, such as the charged scalars lifetimes, EW Precision Observables (EWPOs) and  $h \rightarrow \gamma\gamma$ .

For these additional constraints, we use the results obtained in [10]. In the case of the charged scalars lifetimes, it suffices to take the conservative lower bound of  $m_{H_i^\pm} > 70$  GeV ( $i = 1, 2$ ). All mass ranges in our results where we obtain a correct relic density satisfy this requirement. Furthermore, in our relic density compliant scenarios, there is always a near degeneracy among the charged states and at least one of the neutral scalars, something that helps the model satisfy the EWPOs as well [27, 28, 29, 30].

An interesting portion of parameter space is the one associated with MSSM particles at LEP 2. Those searches can be re-interpreted in terms of the IDM scenario and thus exclude regions of our parameter space as well. In particular, in order to evade the bounds from di-jet and/or di-lepton signals, one must be outside the range of masses where the lightest dark scalar mass is below 80 GeV, the other scalars masses below 100 GeV and their mass differences larger than 8 GeV simultaneously. Again, our results satisfy these criteria.

Regarding constraints coming from  $h \rightarrow \gamma\gamma$ , the inert charged masses and parameters in our analysis fall within the acceptable ranges obtained in Ref. [10] where a combined ATLAS and CMS Run 1 limit was used for the SM-like Higgs signal strengths.

## 6 Conclusions

Motivated by two problems in the SM, from the experimental side, the absence of viable DM candidates, and, from the theoretical side, the lack of an explanation for the three families of matter, we have postulated a 3HDM, wherein two doublets are inert (or dark) and one is active (i.e., with a Higgs nature). This is a configuration that has the advantage, on the one hand, of naturally providing a DM candidate in the form of the lightest inert (pseudo)scalar state and, on the other hand, of potentially explaining the mass hierarchy in the SM fermionic sector between the two lightest generations (connected to the dark sector) and the heaviest one (connected to the active sector). This so-called I(2+1)HDM version of the 3HDM has been repeatedly studied in the literature and shown to be viable against both theoretical constraints and experimental limits in the case in which a  $Z_2$  symmetry is imposed by hand onto the (pseudo)scalar potential, according to which all SM fields, including the active doublet generating the  $Z$ ,  $W^\pm$  and Higgs masses measured by experiment, are even while all those emerging

from the two inert doublets are odd. A consequence of this is that the lightest dark state can be a DM candidate.

In this paper, we have instead adopted a  $Z_3$  symmetry which, in presence of a highly symmetric (pseudo)scalar potential emerging from the dark sector, wherein the two inert doublets share the same Lagrangian parameters, combined with the  $(0, 0, v)$  structure for the doublet VEVs, leads naturally to not only the aforementioned separation between active and inert states but also to a distinction among the latter. In particular, interactions between dark states are such that the lightest member of either inert doublet is stable so that this, in turn, leads to a two-component DM model. In this setup, it is then possible to saturate the relic density of DM with the two DM candidates giving quantitatively comparable contributions to it, which is possible so long that a(n approximate) mass degeneracy exists between the dark charged states. In fact, other configurations can also be generated, where such degeneracy is enforced in the CP-even or CP-odd sector, or else lifted altogether. However, in these cases, one of the two DM components is always dominant in saturating the relic density. Furthermore, all such a dynamics has been obtained in presence of known (in)direct constraints on DM, as well those stemming from EWPOs and collider data, so that we have produced a phenomenologically successful two-component DM model based upon a (pseudo)scalar potential and VEV structure which is theoretically well motivated. Finally, as a byproduct of this analysis, we have also obtained that compliance with the aforementioned experimental results requires the masses of all inert states to be rather light, in fact, at or below the EW scale. Therefore, this ultimately opens the door to the possibility of producing peculiar signals of these dark states at the LHC, all leading to separate cascades terminating with two different DM candidates, which will be the subject of an upcoming publication.

## Acknowledgements

SM is supported in part through the NExT Institute and STFC Consolidated Grant ST/L000296/1. DR-C is supported by the Royal Society Newton International Fellowship NIF/R1/180813. SM and DR-C are also partially supported by the H2020-MSCA-RISE-2014 grant no. 645722 (NonMinimalHiggs). TS and SM are partially supported by the Kogakuin University Grant for the project research "Phenomenological study of new physics models with extended Higgs sector". AA acknowledges support from CONACYT project CB-2015-01/257655 and SNI (México).

## References

- [1] G. Aad *et al.* [ATLAS Collaboration], Phys. Lett. B **716** (2012) 1 [arXiv:1207.7214 [hep-ex]];
- [2] S. Chatrchyan *et al.* [CMS Collaboration], Phys. Lett. B **716** (2012) 30 [arXiv:1207.7235 [hep-ex]].
- [3] G. C. Branco, P. M. Ferreira, L. Lavoura, M. N. Rebelo, M. Sher and J. P. Silva, Phys. Rept. **516** (2012) 1 [arXiv:1106.0034 [hep-ph]].
- [4] P. A. R. Ade *et al.* [Planck Collaboration], Astron. Astrophys. **571** (2014) A16 [arXiv:1303.5076 [astro-ph.CO]].
- [5] N. G. Deshpande and E. Ma, Phys. Rev. D **18** (1978) 2574.
- [6] I. P. Ivanov and E. Vdovin, Eur. Phys. J. C **73** (2013) 2309 [arXiv:1210.6553 [hep-ph]].
- [7] R. Gonzlez Felipe, H. Serdio and J. P. Silva, Phys. Rev. D **87** (2013) no.5, 055010 [arXiv:1302.0861 [hep-ph]].
- [8] I. P. Ivanov and V. Keus, Phys. Rev. D **86** (2012) 016004 [arXiv:1203.3426 [hep-ph]].
- [9] B. Grzadkowski, O. M. Ogreid, P. Osland, A. Pukhov and M. Purmohammadi, JHEP **1106** (2011) 003 [arXiv:1012.4680 [hep-ph]].
- [10] A. Cordero-Cid, J. Hernndez-Snchez, Keus, S. Moretti, D. Rojas and D. Sokolowska, arXiv:1812.00820 [hep-ph].
- [11] V. Keus, S. F. King and S. Moretti, JHEP **1401** (2014) 052 [arXiv:1310.8253 [hep-ph]].
- [12] V. Keus, S. F. King and S. Moretti, Phys. Rev. D **90** (2014) no. 7, 075015 [arXiv:1408.0796 [hep-ph]].
- [13] V. Keus, S. F. King, S. Moretti and D. Sokolowska, JHEP **1411** (2014) 016 [arXiv:1407.7859 [hep-ph]].
- [14] V. Keus, S. F. King, S. Moretti and D. Sokolowska, JHEP **1511** (2015) 003 [arXiv:1507.08433 [hep-ph]].

[15] A. Cordero, J. Hernandez-Sanchez, V. Keus, S. F. King, S. Moretti, D. Rojas and D. Sokolowska, JHEP **1805** (2018) 030 [arXiv:1712.09598 [hep-ph]].

[16] A. Aranda, J. Hernández-Sánchez, R. Noriega-Papaqui and C. A. Vaquera-Araujo, arXiv:1410.1194 [hep-ph].

[17] I. P. Ivanov, V. Keus and E. Vdovin, J. Phys. A **45** (2012) 215201 [arXiv:1112.1660 [math-ph]].

[18] G. Belanger, F. Boudjema, A. Pukhov and A. Semenov, Comput. Phys. Commun. **185** (2014) 960 [arXiv:1305.0237 [hep-ph]].

[19] N. Aghanim *et al.* [Planck Collaboration], arXiv:1807.06209 [astro-ph.CO].

[20] G. Belanger, K. Kannike, A. Pukhov and M. Raidal, JCAP **1204** (2012) 010 [arXiv:1202.2962 [hep-ph]].

[21] C. Karwin, S. Murgia, T. M. P. Tait, T. A. Porter and P. Tanedo, Phys. Rev. D **95** (2017) no. 10, 103005 [arXiv:1612.05687 [hep-ph]].

[22] Q. H. Cao, E. Ma and G. Rajasekaran, Phys. Rev. D **76** (2007) 095011 [arXiv:0708.2939 [hep-ph]].

[23] E. Lundstrom, M. Gustafsson and J. Edsjo, Phys. Rev. D **79** (2009) 035013 [arXiv:0810.3924 [hep-ph]].

[24] A. M. Sirunyan *et al.* [CMS Collaboration], Phys. Lett. B **793** (2019) 520 [arXiv:1809.05937 [hep-ex]].

[25] M. Aaboud *et al.* [ATLAS Collaboration], Phys. Rev. Lett. **122** (2019) no.23, 231801 [arXiv:1904.05105 [hep-ex]].

[26] S. Kanemura, S. Matsumoto, T. Nabeshima and N. Okada, Phys. Rev. D **82** (2010) 055026 [arXiv:1005.5651 [hep-ph]].

[27] G. Altarelli and R. Barbieri, Phys. Lett. B **253** (1991) 161.

[28] M. E. Peskin and T. Takeuchi, Phys. Rev. Lett. **65** (1990) 964.

[29] M. E. Peskin and T. Takeuchi, Phys. Rev. D **46** (1992) 381.

[30] I. Maksymyk, C. P. Burgess and D. London, Phys. Rev. D **50** (1994) 529 [hep-ph/9306267].

- [31] K. Pushkin [LZ Collaboration], Nucl. Instrum. Meth. A **936** (2019) 162.
- [32] G. Arcadi, C. Dring, C. Hasterok and S. Vogl, arXiv:1906.10466 [hep-ph].
- [33] M. Wood *et al.* [Fermi-LAT Collaboration], PoS ICRC **2015** (2016) 1226 [arXiv:1507.03530 [astro-ph.HE]].